Conversion of Alk-1-ynes into Alkyne, Alkynyl, Alkylidyne and Alkylidene Complexes of Molybdenum and Tungsten†

Adrian Hills,[a] David L. Hughes,[a] Neimat Kashef,[a] M. Amelia N. D. A. Lemos,[b] Armando J. L. Pombeiro[b] and Raymond L. Richards*,[a]
[a] *AFRC-IPSR Nitrogen Fixation Laboratory, University of Sussex, Falmer, Brighton BN1 9RQ, UK*
[b] *Centro de Química Estrutural, Complexo I Instituto Superior Técnico, Av. Rovisco Pais, 1096 Lisbon Codex, Portugal*

A variety of alkyne, alkynyl, alkylidyne and alkylidene complexes has been obtained from the alkynes $RC{\equiv}CH$ (R = Ph, CO_2Me or CO_2Et). The reactions of these alkynes with *trans*-$[M(N_2)_2(dppe)_2]$ (M = Mo or W, dppe = $Ph_2PCH_2CH_2PPh_2$) and *trans*-$[Mo(N_2)_2(depe)_2]$ (depe = $Et_2PCH_2CH_2PEt_2$) give the alkyne complex $[Mo(HC{\equiv}CPh)_2(dppe)_2]$ **A**, the alkynyl complexes $[MH_2(C{\equiv}CR)_2(L\text{–}L)_2]$ **B** (M = Mo or W; R = Ph, CO_2Me or CO_2Et; L–L = dppe; M = Mo, R = Ph, L–L = depe) and *trans*-$[M(C{\equiv}CR)_2(dppe)_2]$ **C** (M = Mo or W; R = Ph, CO_2Me or CO_2Et) depending on the conditions. The redox properties and interconversion of **B** and **C** are described and the X-ray crystal structures of **B** (M = W, R = CO_2Me, L–L = dppe) and **C** (M = Mo, R = Ph) are presented. The complexes $[WH_2(C{\equiv}CR)_2(dppe)_2]$ **B** (R = CO_2Me or Ph) react with HBF_4 to give $[WF({\equiv}CCH_2CO_2Me)(dppe)_2]$ **D** and $[WF({=}CHCH_2Ph)(dppe)_2]BF_4$ **E** respectively. The polymerisation of $RC{\equiv}CH$ (R = H or Ph) at these metal centres is also discussed.

The binding and reactions of alkynes at mononuclear metal centres are increasingly being studied not only because of the ability of alkynes to transform, *e.g. via* polymerisation or coupling reactions, into carbon species of potential use,[1] but also because the reduction of acetylene to ethylene is an important probe of the active metallic centre in the enzyme nitrogenase.[2a]

We have been studying the reactions of the alternative substrates of nitrogenase, in particular alkynes, at dinitrogen-binding sites.[2b] In this paper we describe the transformation of alkynes $RC{\equiv}CH$ (R = H, CO_2Me, CO_2Et or Ph) which occur at the dinitrogen-binding centres $\{M(dppe)_2\}$ (dppe = $Ph_2PCH_2CH_2PPh_2$). Some of this work has already been reported in preliminary form[3] and related work with iron- and cobalt-dinitrogen complexes has been described recently.[4]

Results and Discussion

Alkyne Complexes.—As is detailed below, the general result of treating *trans*-$[M(N_2)_2(dppe)_2]$ with $RC{\equiv}CH$ is the formation of alkynyl and derived complexes with concomitant oxidation of the metal centre, these compounds being formed presumably by transformation of a precursor alkyne complex. In one case we have been able to isolate an example of such a complex. Treatment of *trans*-$[Mo(N_2)_2(dppe)_2]$ with $PhC{\equiv}CH$ in tetrahydrofuran (thf) under argon gave the diamagnetic yellow compound *trans*-$[Mo(HC{\equiv}CPh)_2(dppe)_2]$ **A**. Its characterisation follows from the physical properties shown in Table 1, in particular the presence of the $HC{\equiv}CPh$ ligand is defined by the ^{13}C NMR data. The CH ^1H resonance is probably obscured by Ph resonances and no $C{\equiv}C$ stretching IR band could be observed; this is not surprising as these bands are generally weak.[5] In all these preparations a competing reaction was polymerisation of the alkyne *e.g.* to give the bright red polymer of $PhC{\equiv}CH$. We were not able to define conditions to eliminate this process, indeed when we attempted to study the reactions of $HC{\equiv}CH$ the only product was a black precipitate, identified by IR bands at 1560 and 1610 cm^{-1} as polyacetylene.[6] Use of relatively low reaction temperatures and avoidance of irradiation reduced the formation of polyphenylacetylene, whereas treatment of *trans*-$[Mo(N_2)_2(dppe)_2]$ with $PhC{\equiv}CH$ in thf for 7 d under tungsten-light irradiation gave polyphenylacetylene as the only isolated product.

Alkynyl Complexes.—As noted above, the dominant reaction observed when *trans*-$[M(N_2)_2(L\text{–}L)_2]$ (L–L = diphosphine) are treated with $RC{\equiv}CH$ is oxidation of the metal, with the formation of alkynyl complexes. These compounds fall into two classes, $[MH_2(C{\equiv}CR)_2(L\text{–}L)_2]$ **B** and *trans*-$[M(C{\equiv}CR)_2(dppe)_2]$ **C**. It is difficult to define the conditions necessary to isolate exclusively particular complexes of this series since their formation depends subtly upon the various substituents and upon reaction conditions; we give in the Experimental section what in our experience are the conditions most likely to give a high yield of the particular type of complex. The interconversion of **B** and **C** has been studied in some detail by electrochemistry and is discussed below. The formulation and structures of complexes **B** and **C** follows from their physical properties (Table 1) and structural characterisation of $[WH_2(C{\equiv}CCO_2Me)_2(dppe)_2]$ and *trans*-$[Mo(C{\equiv}CPh)_2(dppe)_2]$ by X-ray crystallography.

Although we have no detailed mechanistic information for these systems, it is most likely that the initial step in these reactions is loss of N_2 from the metal centre, since this requires irradiation for tungsten but not for molybdenum[7] and it is necessary to irradiate with tungsten light to initiate the reactions of alkynes with *trans*-$[W(N_2)_2(dppe)_2]$ but not for the molybdenum analogue. After loss of N_2 the next step most likely is addition of alkyne to give compounds **A** which then undergo oxidative addition to give **B** (Scheme 1). Thereafter loss of H_2 will give compounds **C**. This reaction sequence would appear to be related to that observed in the reaction of RSH with *trans*-$[Mo(N_2)_2(dppe)_2]$ which has been studied in detail.[8]

---

† *Supplementary data available:* see Instructions for Authors, *J. Chem. Soc., Dalton Trans.*, 1992, Issue 1, pp. xx–xxv.

Table 1 Physical properties of molybdenum and tungsten complexes

Compound[a]	Colour and yield (%)	Analysis (%)[b]		Infrared[c]	NMR[d]		
		C	H	(cm^{-1})	^{1}H	^{31}P-{^{1}H}	^{13}C-{^{1}H}
[Mo(HCCPh)$_2$(dppe)$_2$]	Yellow (69)	74.2 (74.4)	5.7 (5.5)	—	7.3–6.6 (m, 50, C$_6$H$_5$) 1.8 (m, 8, PCH$_2$)	−76 (s, *trans*-dppe)	151 (H*C*CPh[e]) 121 (HC*C*Ph)
[MoH$_2$(C$_2$Ph)$_2$(depe)$_2$]	Brown (50)	59.9 (60.6)	8.3 (8.4)	2040[f]	7.0–6.0 (m, 5, C$_6$H$_5$) 1.95–1.52 (m, 24, PCH$_2$ + $\mathrm{C}\mathit{H}_2\mathrm{CH_3}$) 1.52–1.21 (t, 24, $\mathrm{CH_2C}\mathit{H}_3$) −6.3 (qnt, 2,[g] MoH$_2$)	−76.4 (m, *trans*-depe)	138 (s, *C*CPh) 130–123 (m, C$_6$H$_5$) 113 (s, C*C*Ph) 23.0–20.2 (m, $\mathit{C}\mathrm{H_2CH_3}$) 20.9–19.0 (m, PCH$_2$) 9.3–8.8 (m, $\mathrm{CH_2}\mathit{C}\mathrm{H_3}$)
[WH$_2$(C$_2$Ph)$_2$(dppe)$_2$]	Orange (60)	68.5 (68.9)	5.4 (5.1)	2040[f]	7.9–7.0 (m, 50, C$_6$H$_5$) 2.3–2.4 (br s, 8, PCH$_2$) −1.4 (m, 2, WH$_2$)	−92.6 (s) −112.2 (s)	139 (s, *C*CPh) 130–123 (m, C$_6$H$_5$) 114 (s, C*C*Ph) 19.0–21.0 (m, PCH$_2$)
[WH$_2$(C$_2$CO$_2$Me)$_2$(dppe)$_2$]	Orange (62)	62.8 (62.7)	5.0 (4.8)	2040[f] 1650[h]	8.1–7.0 (m, 40, C$_6$H$_5$) 5.27 (s, 6, CCH$_3$) 2.6–2.1 (m, 8, PCH$_2$) −1.3 (m, 2, WH$_2$)	−93.2 (s) −111.5 (s)	153 (s, C*C*O$_2$Me) 141 (s, W*C*C) 140.9–127.5 (m, C$_6$H$_5$) 112 (s, WC*C*) 26.0 (s, PCH$_2$) 15.0 (s, OCH$_3$)
[WH$_2$(C$_2$CO$_2$Et)$_2$(dppe)$_2$]	Orange (60)	63.9 (63.4)	4.9 (5.1)	2040[f] 1660[h]	7.7–7.0 (m, 40, C$_6$H$_5$) 3.6 (q, 4, $\mathrm{C}\mathit{H}_2\mathrm{CH_3}$) 2.6–2.1 (m, 8, PCH$_2$) 1.2 (t, 6, $\mathrm{CH_2C}\mathit{H}_3$) −1.5 (m, 2, WH$_2$)	−91.5 (s) −98.4 (s)	167 (s, CC*C*O$_2$Et) 147 (s, W*C*C) 140.8–128.9 (m, C$_6$H$_5$) 125 (s, WC*C*) 33 (s, OCH$_2$) 26 (s, PCH$_2$) 14 (s, $\mathrm{CH_2}\mathit{C}\mathrm{H_3}$)
[Mo(C$_2$Ph)$_2$(dppe)$_2$]	Red (74)	73.2 (73.4)	6.0 (5.9)	2020[f]	8.0–7.0 (m, 50, C$_6$H$_5$) 2.14–2.04 (m, 8, PCH$_2$)	−74.6 (s, *trans*-dppe)	142 (br s, Mo*C*C) 134.4–121.4 (m, C$_6$H$_5$) 115 (s, MoC*C*) 26.51 (s, PCH$_2$)
[Mo(C$_2$CO$_2$Me)$_2$(dppe)$_2$]	Orange (65)	67.1 (67.8)	5.4 (5.3)	2000[f] 1675[h]	8.2–7.0 (m, 40, C$_6$H$_5$), 3.5 (s, 6, CH$_3$) 2.2–2.0 (m, 8, PCH$_2$)	−78 (s, *trans*-dppe)	144.2 (br s, Mo*C*C) 132–127 (m, C$_6$H$_5$) 116 (s, MoC*C*) 30.3 (s, CH$_3$) 25 (s, PCH$_2$)
[Mo(C$_2$CO$_2$Et)$_2$(dppe)$_2$]	Orange (67)	68.1 (68.3)	5.4 (5.3)	2000[f] 1675[h]	7.5–7.0 (m, 40, C$_6$H$_5$) 3.55 (q, 4, $\mathrm{C}\mathit{H}_2\mathrm{CH_3}$) 2.1 (br, 8, PCH$_2$) 1.24 (t, 6, $\mathrm{CH_2C}\mathit{H}_3$)	−75 (s, *trans*-dppe)	142 (br s, Mo*C*C) 132–127 (m, C$_6$H$_5$) 118 (s, MoC*C*) 30 (s, OCH$_2$) 25 (s, PCH$_2$) 14 (s, $\mathrm{CH_2}\mathit{C}\mathrm{H_3}$)
[W(C$_2$Ph)$_2$(dppe)$_2$]	Orange (64)	68.5 (68.9)	5.4 (5.1)	2040[f]	8.4–7.1 (m, 50, C$_6$H$_5$) 2.32 (br s, 8, PCH$_2$)	−93.5 (s[i], *trans*-dppe)	139.2 (s, W*C*C) 138–126 (m, C$_6$H$_5$) 113.0 (s, WC*C*) 25.2 (s, PCH$_2$)
[W(C$_2$CO$_2$Me)$_2$(dppe)$_2$]	Orange (65)	62.1 (62.7)	4.8 (4.8)	2040[f]	7.7–7.2 (m, 40, C$_6$H$_5$) 3.6–3.1 (br s, 8, PCH$_2$) 2.4 (s, 6, CH$_3$)	−108 (s, *trans*-dppe)	—
[W(C$_2$CO$_2$Et)$_2$(dppe)$_2$]	Orange (60)	63.7 (63.4)	5.2 (5.1)	2040[f] 1675[h]	7.3–7.2 (m, 40, C$_6$H$_5$) 3.69 (q, 4, $\mathrm{C}\mathit{H}_2\mathrm{CH_3}$) 2.1 (br s, 8, PCH$_2$) 1.32 (t, 6)	−90.85 (s, *trans*-dppe)	147 (s, W*C*C) 138–127 (m, C$_6$H$_5$) 126 (s, WC*C*) 33 (s, OCH$_2$) 26 (s, PCH$_2$) 14 (s, $\mathrm{CH_2}\mathit{C}\mathrm{H_3}$)
[WF(≡CCH$_2$CO$_2$Me)(dppe)$_2$]	Green (39)	61.3 (62.0)	5.0 (4.7)	—	6.7 (m, 40, C$_6$H$_5$) 3.74 (s, 2, $\mathrm{C}\mathrm{C}\mathit{H}_2$-CO$_2$Me) 3.4 (s, 3, CH$_3$) 2.5 (br s, 8, PCH$_2$) 141.3 (qnt,[k,l] WF)	−107.12 (d,[j] *trans*-dppe)	291 (br, M≡*C*CH$_2$-CO$_2$Me) 167 (s, *C*O$_2$Me) 128–138 (m, C$_6$H$_5$) 44.7 (s,[m] $\mathrm{C}\mathit{C}\mathrm{H_2}$-CO$_2$Me) 29.6 (s, PCH$_2$) 25 (s, OCH$_2$) 14 (s, $\mathrm{CH_2}\mathit{C}\mathrm{H_3}$)

Table 1 (*continued*)

		Analysis (%)[b]			NMR[d]		
Compound[a]	Colour and yield (%)	C	H	Infrared[c] (cm^{-1})	^{1}H	^{31}P-{^{1}H}	^{13}C-{^{1}H}
[WF(=CHCH$_2$Ph)(dppe)$_2$]BF$_4$	Orange (40)	59.5 (60.5)	5.0 (4.7)	—	7–6 (m, 45, C$_6$H$_5$) 5.35 (t, 1,[m] C*H*CH$_2$Ph) 4.26 (d, 2,[m] CHC*H*$_2$Ph) 2.72 (br, 8, PCH$_2$) −97.3 (qnt.[l,n], WF) −156.9 (s,[l] BF$_4^-$)	−109.1 (d,[n] *trans*-dppe)	251.8 (s,[o] W*C*HCH$_2$Ph) 134.2–128 (m, C$_6$H$_5$) 58.3 (s,[p] CH*C*H$_2$Ph) 27.3 (s, PCH$_2$)

[a] *trans* Configuration except for [MH$_2$(C≡CR)$_2$(dppe)$_2$] complexes, see text. [b] Calc. values in parentheses. [c] In KBr pellets, all bands strong. [d] In CD$_2$Cl$_2$; ^{1}H and ^{13}C relative to SiMe$_4$, ^{19}F relative to CFCl$_3$, ^{31}P relative to P(OMe)$_3$; s = singlet, d = doublet, t = triplet, q = quartet, qnt = quintet, m = multiplet, br = broad; relative integration in parentheses. [e] Doublet in proton-coupled spectrum, $^1J(^{13}C^1H)$ = 154.4 Hz. [f] ν(C≡C). [g] $^2J(^{31}P^1H)$ = 46.5 Hz. [h] ν(C≡O). [i] Tungsten satellites, $J(^{187}W^{31}P)$ = 322 Hz. [j] $^3J(^1H^1H)$ = 7.3 Hz. [k] ^{19}F resonance. [l] $^2J(^{31}P^{19}F)$ = 35.2 Hz. [m] Triplet in proton-coupled spectrum, $^1J(^{13}C^1H)$ = 120 Hz. [n] $^2J(^{31}P^{19}F)$ = 34 Hz. [o] Doublet in proton-coupled spectrum, $^1J(^{13}C^1H)$ = 154.9 Hz. [p] Triplet in undecoupled spectrum, $^1J(^{13}C^1H)$ = 144 Hz.

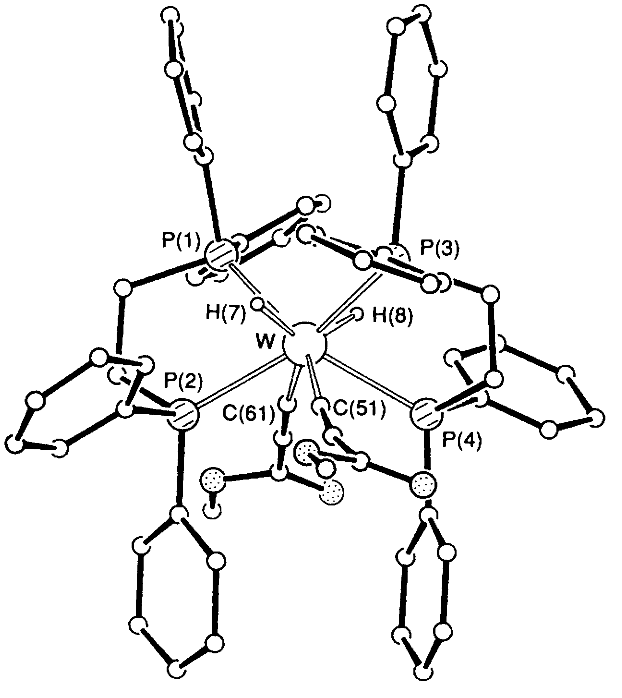

Fig. 1 Molecular structure of the complex [WH$_2$(C≡CCO$_2$Me)$_2$(dppe)$_2$]·thf

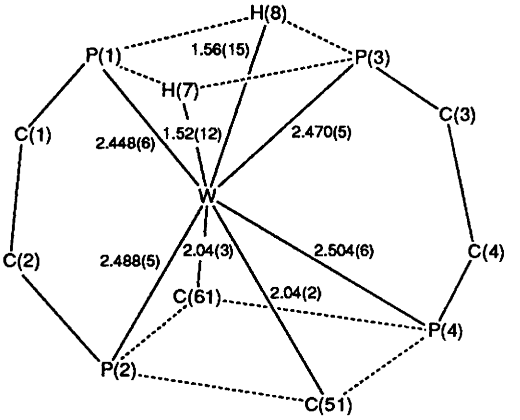

Fig. 2 Square-antiprismatic co-ordination at tungsten in [WH$_2$(C≡C-CO$_2$Me)$_2$(dppe)$_2$]·thf

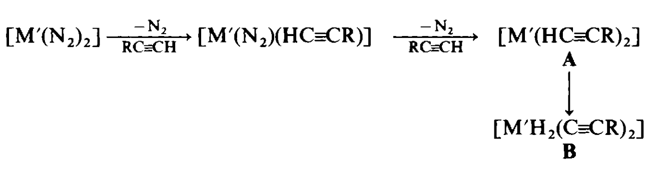

Scheme 1 M′ = M(L–L)$_2$; R = Ph, CO$_2$Me or CO$_2$Et

Structure of Compounds **B**.—These red-orange, diamagnetic complexes show characteristic ν(C≡C) values in the range 2000–2040 cm^{-1} and high-field hydride resonances. For **B** (M = W) the ^{31}P NMR pattern is a deceptively simple doublet but [MoH$_2$(C≡CPh)$_2$(depe)$_2$] (depe = Et$_2$PCH$_2$CH$_2$PEt$_2$) gives a complex multiplet which was not analysed in detail. The structure of these complexes has been established by X-ray crystallography for [WH$_2$(C≡CCO$_2$Me)$_2$(dppe)$_2$] as shown in Fig. 1 and detailed in Tables 2 and 3. Although rapid deterioration of the crystal during data collection limited the extent of refinement and thus the total accuracy of the structure, nevertheless the hydride ligands could be located with reasonable certainty and the geometry is established as having the tungsten atom in the centre of a square antiprism with a pseudo-two-fold axis relating ligands in pairs. Each of the phosphine ligands has one phosphorus atom in each square face of the antiprism. The hydride ligands have a *cis* arrangement and are in reasonable locations at opposite corners of one square face of the antiprism. The ligating alkynyl C atoms are at opposite corners of the other square face (Fig. 2) and are bonded almost symmetrically to the tungsten atom, with W–C bonds almost equal within the limits of experimental error, 2.039(1) Å (Table 2). The C≡C bond distances, mean 1.23(1) Å, are slightly longer than in free ethyne (1.205 Å) and lie within the normal range found in alkynyl complexes (1.19–1.25 Å).[9] The W–H bond distances [1.52(12) and 1.56(15) Å] are in the range of other observed metal–hydrogen distances.[10]

The two common structures for eight-co-ordinate complexes are the square antiprism (*SAPR*) and the dodecahedron (*DD*). A number of related hydride complexes which have phosphine ligands have the *DD* structure, *e.g.* [MoH$_4$(dppe)$_2$],[11] [MoH$_3$(C≡CBu^t)(dppe)$_2$],[12] [MoH$_2$Cl$_2$(dppe)$_2$],[13] [MoH$_4$(PMePh$_2$)$_4$],[14] [WH$_4$(PEtPh$_2$)$_4$][15] and [WH$_2$Cl$_2$(PMe$_2$Ph)$_4$].[16] The energy difference between the *SAPR* and *DD* structures is small[17] and the relatively large bulk of the two C≡CCO$_2$Me ligands might be responsible for the adoption of the *SAPR* geometry in the case of [WH$_2$(C≡CCO$_2$Me)$_2$(dppe)$_2$].

Structure of Compounds **C**.—The orange, diamagnetic complexes **C** are formed from **B** by loss of dihydrogen (see below) and it is not unexpected that these are the predominant species isolated from reactions of *trans*-[Mo(N$_2$)$_2$(dppe)$_2$],

Table 2 Selected molecular dimensions in $[WH_2(C\equiv CCO_2Me)_2(dppe)_2]\cdot thf$. Bond lengths are in Å, angles in °. Estimated standard deviations (e.s.d.s) are in parentheses

(*a*) About the W atom			
W–P(1)	2.448(6)	W–C(51)	2.038(21)
W–P(2)	2.488(5)	W–C(61)	2.041(25)
W–P(3)	2.470(5)	W–H(7)	1.52(12)
W–P(4)	2.504(6)	W–H(8)	1.56(15)
P(1)–W–P(2)	80.7(2)	C(51)–W–C(61)	116.0(8)
P(1)–W–P(3)	102.3(2)	P(1)–W–H(7)	71.3(35)
P(2)–W–P(3)	145.2(2)	P(2)–W–H(7)	73.8(31)
P(1)–W–P(4)	141.9(2)	P(3)–W–H(7)	74.5(31)
P(2)–W–P(4)	119.7(2)	P(4)–W–H(7)	142.1(33)
P(3)–W–P(4)	79.2(2)	C(51)–W–H(7)	76.5(36)
P(1)–W–C(51)	145.3(7)	C(61)–W–H(7)	137.7(32)
P(2)–W–C(51)	78.2(6)	P(1)–W–H(8)	78.0(46)
P(3)–W–C(51)	80.9(5)	P(2)–W–H(8)	136.9(39)
P(4)–W–C(51)	72.7(7)	P(3)–W–H(8)	76.4(40)
P(1)–W–C(61)	81.5(6)	P(4)–W–H(8)	65.2(47)
P(2)–W–C(61)	70.2(6)	C(51)–W–H(8)	135.0(45)
P(3)–W–C(61)	144.5(6)	C(61)–W–H(8)	69.9(41)
P(4)–W–C(61)	77.0(7)	H(7)–W–H(8)	131.5(58)
(*b*) In the alkynyl ligand			
C(51)–C(52)	1.22(3)	C(61)–C(62)	1.24(4)
C(52)–C(53)	1.40(4)	C(62)–C(63)	1.41(6)
C(53)–O(54)	1.23(4)	C(63)–C(64)	1.20(6)
C(53)–O(55)	1.40(4)	C(63)–O(65)	1.25(4)
O(55)–C(56)	1.37(3)	O(65)–C(66)	1.43(4)
W–C(51)–C(52)	172.8(16)	W–C(61)–C(62)	174.5(20)
C(51)–C(52)–C(53)	168.5(23)	C(61)–C(62)–C(63)	175.9(24)
C(52)–C(53)–O(54)	132.7(28)	C(62)–C(63)–O(64)	125.6(34)
C(52)–C(53)–O(55)	111.2(26)	C(62)–C(63)–O(65)	115.1(41)
O(54)–C(53)–O(55)	115.8(23)	O(64)–C(63)–O(65)	119.3(41)
C(53)–O(55)–C(56)	119.3(21)	C(63)–O(65)–C(66)	113.3(32)

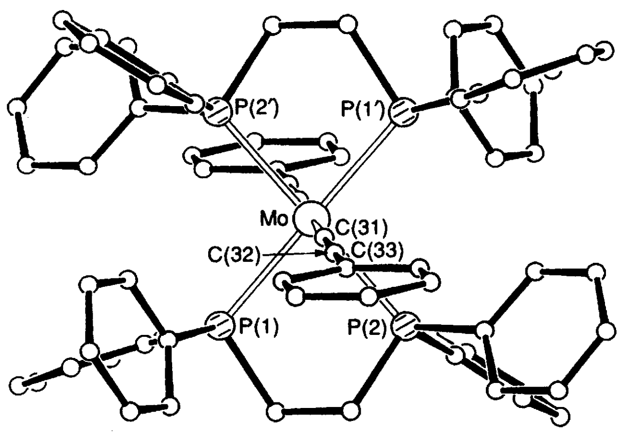

Fig. 3 Molecular structure of the complex *trans*-$[Mo(C\equiv CPh)_2(dppe)_2]\cdot 2thf$

since Mo–H are generally more labile than W–H bonds. Irradiation is necessary to initiate loss of H_2 from compounds **B** (M = W). For molybdenum complexes only *trans*-$[Mo(N_2)_2(depe)_2]$ yields a hydride–alkynyl complex; presumably the greater electron-releasing ability of the depe ligand aids the stability of the Mo–H bond in this case.

The *trans* structure assigned to compounds **C** follows from their singlet ^{31}P NMR resonance and single $\nu(C\equiv C)$ stretching band in the IR spectrum and is defined by the X-ray structure of *trans*-$[Mo(C\equiv CPh)_2(dppe)_2]$ shown in Fig. 3 with structural details in Tables 4 and 5. In this structure, the molybdenum atom lies on a crystallographic centre of symmetry and its co-ordination geometry is essentially *trans*-octahedral. The virtually linear alkynyl groups are approximately 11° away from the normal to the plane of the four P atoms, and each of the four phosphine phenyl groups on that side of the molecule has close contacts with the $C\equiv C$ group. The phenyl groups of the alkynyl ligands extend out of the molecule well beyond the phosphine ligands. There is only one other structurally characterised mononuclear alkynyl complex of molybdenum, $[MoH_3(C\equiv CBu^t)(dppe)_2]$[12] [$d(C\equiv C)$ 1.209(14) Å], and only one similarly defined tungsten complex, $[W(C_5H_5)(C\equiv CC_3H_5)(CO)_2(PMe_3)]$ [$d(C\equiv C)$ 1.205(15) Å].[18] The $C\equiv C$ distance in $[Mo(C\equiv CPh)_2(dppe)_2]$ of 1.24(1) Å is longer than these distances, also than that of free acetylene (1.205 Å) and indeed is at the longer end of the range observed in alkynyl complexes of Mo and W (1.19–1.25 Å).[9] {The $C\equiv C$ distance of $[WH_2(C\equiv CCO_2Me)_2(dppe)_2]$ is similar but because of the low accuracy of that structure, there can be no detailed comparison}. The lengthening of the $C\equiv C$ distance in *trans*-$[Mo(C\equiv CPh)_2(dppe)_2]$ is balanced by a slight shortening of the M–C bond to 2.093(8) Å, compared to 2.175(10) Å in $[MoH_3(C\equiv CBu^t)(dppe)_2]$[12] and 2.134(11) Å in $[W(C_5H_5)(C\equiv CC_3H_5)(CO)_2(PMe_3)]$.[18]

The Mo–C bond therefore appears to have a bond order of rather greater than one; for comparison we note that in $[W(CH_2CMe_3)(=CHCMe_3)(\equiv CCMe_3)(Me_2PCH_2CH_2PMe_2)]$[19] the W–C(alkyl) single-bond distance is 2.258(9) Å and the W=C(alkylidene) double-bond distance is 1.942(9) Å. The relatively short Mo–C distance observed in *trans*-$[Mo(C\equiv CPh)_2(dppe)_2]$ is not unexpected in view of the established strong π-electron release from the $\{Mo(dppe)_2\}$ site.

Interconversion and Redox Properties of Compounds **B** *and* **C**.—The half-wave redox potentials and other properties of these compounds are collected in Table 6. At a platinum electrode in 0.2 mol dm^{-3} $[NBu_4][BF_4]$–thf, compounds *trans*-$[M(C\equiv CR)_2(dppe)_2]$ **C** (M = Mo) show a reversible single-electron oxidation at $^{I}E_{\frac{1}{2}}^{ox}$ values in the range 0 to −0.12 V (*versus* saturated calomel electrode SCE), depending upon the substituent; this is followed at a higher potential ($^{II}E_p^{ox}$ of 0.69–0.88 V) by a second, irreversible, anodic process. Reduction waves are also seen (Table 6). The $^{I}E_{\frac{1}{2}}^{ox}$ values are close to that observed for *trans*-$[MoCl_2(dppe)_2]$ (−0.05 V)[20] indicating a similar electronic behaviour of the $C\equiv CR^-$ and Cl^- ligands towards this metal centre. This analogy also extends to $[W(C\equiv CPh)_2(dppe)_2]$ **C** (M = W) (−0.29 V) and *trans*-$[WCl_2(dppe)_2]$ (−0.24 V).[20] The hydride compound $[WH_2(C\equiv CCO_2Me)_2(dppe)_2]$ **B** (M = W) has $^{I}E_{\frac{1}{2}}^{ox}$ at −0.02 V which compares with $[WH_2Cl_2(dppe)_2]$ (−0.07 V).[20]

The conversion of $[WH_2(C\equiv CPh)_2(dppe)_2]$ into *trans*-$[W(C\equiv CPh)_2(dppe)_2]$ was monitored by electrochemistry; the wave corresponding to the dihydride disappeared under tungsten light irradiation at 20 °C in thf during 6 h, with the concomitant appearance of a wave assigned to $[W(C\equiv CPh)_2(dppe)_2]$, equation (1). This reaction is not reversible; under the electrochemical conditions the product did not react with dihydrogen at 1 atm (101 325 Pa) pressure.

$$[WH_2(C\equiv CPh)_2(dppe)_2] \xrightarrow{thf,\,h\nu} [W(C\equiv CPh)_2(dppe)_2] + H_2 \quad (1)$$

Reactions of Compounds **B** *and* **C** *with* HBF_4.—*Formation of trans*-$[WF(\equiv CCH_2CO_2Me)(dppe)_2]$ **D**. Addition of $[Et_2OH][BF_4]$ to a solution of $[WH_2(C\equiv CCO_2Me)_2(dppe)_2]$ **B** in thf at 20 °C gives a moderately air-stable, diamagnetic, green complex **D**. Compound **D** is formulated as an alkylidyne complex, as shown in Scheme 2, on the basis of the following data (see also Table 1). It shows a quintet in its ^{19}F NMR spectrum and a doublet [$J(^{19}F^{31}P)$ = 35.2 Hz] in its ^{31}P NMR spectrum, defining the *trans*-$\{WF(dppe)_2\}$ unit. Its ^{13}C NMR spectrum shows, among others, a low-field resonance (δ 291) in the region (230–320) characteristic of alkylidyne complexes such as *trans*-$[ReF(\equiv CCH_2Bu^t)(dppe)_2]BF_4$,[21] $[WX(\equiv CCH_2Ph)$-

Table 3 Final atomic coordinates (fractional × 10^4) for $[WH_2(C{\equiv}CCO_2Me)_2(dppe)_2]{\cdot}thf$ with e.s.d.s in parentheses

Atom	*x*	*y*	*z*
W	4756.7(8)	2353.3(4)	1007.6(7)
C(11a)	3754(17)	1029(9)	2743(16)
C(12a)	3856(19)	1387(10)	3744(17)
C(13a)	2923(21)	1200(11)	4317(19)
C(14a)	1943(23)	735(11)	3927(20)
C(15a)	1839(23)	402(12)	2994(21)
C(16a)	2758(19)	538(10)	2363(17)
C(11b)	6255(19)	1147(10)	2821(17)
C(12b)	7307(24)	1334(11)	2515(21)
C(13b)	8404(27)	1183(12)	3112(23)
C(14b)	8283(27)	851(12)	4048(23)
C(15b)	7290(25)	624(12)	4304(21)
C(16b)	6190(23)	761(11)	3722(19)
P(1)	4876(5)	1316(3)	1914(4)
C(1)	4633(16)	644(8)	836(14)
C(2)	3722(16)	730(8)	−248(14)
P(2)	4161(5)	1576(3)	−690(4)
C(21a)	2939(19)	1640(10)	−1831(16)
C(22a)	3040(21)	2186(11)	−2422(18)
C(23a)	2050(21)	2257(12)	−3361(19)
C(24a)	1074(22)	1777(12)	−3588(19)
C(25a)	974(27)	1232(15)	−3054(23)
C(26a)	1908(24)	1169(13)	−2132(21)
C(21b)	5292(18)	1471(9)	−1482(16)
C(22b)	6466(20)	1786(10)	−1156(17)
C(23b)	7357(23)	1684(11)	−1736(20)
C(24b)	6914(22)	1267(10)	−2680(18)
C(25b)	5790(22)	961(11)	−3019(19)
C(26b)	4956(21)	1049(10)	−2427(18)
C(31a)	7092(20)	2957(9)	3660(17)
C(32a)	8286(22)	2941(10)	3951(20)
C(33a)	8744(27)	2785(12)	5100(24)
C(34a)	8015(25)	2678(11)	5814(24)
C(35a)	6847(24)	2695(11)	5530(21)
C(36a)	6394(21)	2855(10)	4423(19)
C(31b)	7711(17)	3485(10)	1637(15)
C(32b)	8029(19)	4154(10)	1425(16)
C(33b)	8980(22)	4382(13)	892(19)
C(34b)	9581(21)	3954(12)	572(18)
C(35b)	9282(22)	3292(12)	782(18)
C(36b)	8296(20)	3055(11)	1263(17)
P(3)	6422(5)	3160(3)	2233(5)
C(3)	5868(16)	3888(8)	2528(14)
C(4)	5060(16)	4070(8)	1502(15)
P(4)	3838(5)	3333(3)	1035(5)
C(41a)	2905(18)	3542(9)	−232(15)
C(42a)	1761(20)	3202(10)	−556(17)
C(43a)	998(22)	3305(11)	−1543(19)
C(44a)	1432(22)	3788(11)	−2208(20)
C(45a)	2609(22)	4124(11)	−1953(20)
C(46a)	3334(21)	4002(10)	−936(18)
C(41b)	2907(17)	3357(10)	2078(15)
C(42b)	2588(18)	2852(10)	2731(17)
C(43b)	1936(20)	2905(12)	3547(19)
C(44b)	1587(20)	3477(11)	3636(19)
C(45b)	1859(19)	4006(11)	2968(18)
C(46b)	2544(18)	3932(10)	2158(17)
C(51)	5295(18)	2957(10)	−179(17)
C(52)	5737(18)	3340(11)	−804(17)
C(53)	6322(24)	3868(16)	−1328(21)
O(54)	6327(14)	4460(8)	−1321(13)
O(55)	7122(14)	3670(7)	−1891(12)
C(56)	7849(25)	4135(13)	−2376(23)
C(61)	2969(23)	1931(10)	715(16)
C(62)	1880(30)	1712(11)	611(16)
C(63)	654(45)	1452(21)	574(27)
O(64)	−9(18)	1745(10)	868(21)
O(65)	261(15)	867(10)	188(16)
C(66)	−960(28)	607(14)	243(25)
H(7)	5893(96)	2158(44)	862(76)
H(8)	4274(112)	2448(58)	2075(113)

Disordered thf molecules; each atom has a site occupancy factor of 0.5

Atom	*x*	*y*	*z*
C(101)	6114(78)	5436(33)	4063(80)
C(102)	5838(528)	4786(164)	4595(591)
C(103)	4853(40)	4800(16)	5201(36)
C(104)	4580(44)	5471(21)	5041(46)
C(105)	5346(42)	5867(15)	4342(36)
C(201)	−1147(33)	4706(24)	5000(52)
C(202)	−157(56)	4770(30)	6026(34)
C(203)	1009(37)	4911(25)	5659(50)
C(204)	734(54)	5035(42)	4438(54)
C(205)	−582(59)	4751(28)	4010(32)

Table 4 Selected bond lengths (Å) and angles (°) in *trans*-$[Mo(C{\equiv}CPh)_2(dppe)_2]{\cdot}2thf$ with e.s.d.s in parentheses

(*a*) About the Mo atom			
Mo–P(1)	2.501(2)	P(1)–Mo–P(2)	79.8(1)
Mo–P(2)	2.514(2)	P(1)–Mo–C(31)	86.7(3)
Mo–C(31)	2.093(8)	P(2)–Mo–C(31)	79.1(2)
(*b*) In the alkynyl ligand			
C(32)–C(32)	1.237(12)	Mo–C(31)–C(32)	175.6(7)
C(32)–C(33)	1.422(12)	C(31)–C(32)–C(33)	177.8(9)

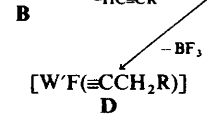

Scheme 2 R = CO_2Me, W′ = $W(dppe)_2$

$(CO)_2(dppe)_2]$ (X = Me_2CO, PMe_3 or H_2O) and related compounds.^{22} This resonance was unchanged in the proton-coupled spectrum. Other assignments are in Table 1.

The mechanism of the formation of compound **D** clearly is complicated and detailed studies are necessary to understand it, but a reasonable suggestion can be made, as in Scheme 2, which is consistent with published observations by ourselves and others on related systems^{21,22} and with the observations made in this study. Loss of alkyne from $[WH_2(C{\equiv}C\text{-}CO_2Me)_2(dppe)_2]$ must occur in the formation of **D**. Protonation of the β-carbon of the remaining alkynyl ligand would give a vinylidene ligand, followed by a second β protonation to give the alkylidyne ligand. Although we could not detect any intermediates, β protonation of alkynyl and vinylidene ligands is well established in other studies.^{21,22} The addition of fluoride to the metal from BF_4^- is also well documented in molybdenum^{23} and related rhenium^{21} chemistry.

Formation of trans-$[WF(CHCH_2Ph)(dppe)_2]BF_4$ **E**. The reaction of $[WH_2(C{\equiv}CPh)_2(dppe)_2]$ with $[Et_2OH][BF_4]$ in thf under similar conditions to the reaction of Scheme 2 gave a diamagnetic, moderately air-stable, orange compound **E** formulated as an alkylidene complex as follows. Compound **E** is a 1:1 electrolyte in $MeNO_2$ and the *trans*-$\{WF(dppe)_2\}BF_4$ unit in its structure is defined by its ^{19}F and ^{31}P NMR data (Table 1). Its ^{13}C NMR spectrum shows a low-field resonance (δ 251.8) which splits into a doublet in the proton-coupled spectrum, characterising the alkylidene carbon; the ^1H NMR

Table 5 Final atomic coordinates (fractional $\times 10^4$) for *trans*-[$Mo(C{\equiv}CPh)_2(dppe)_2$]·2thf with e.s.d.s in parentheses

Atom	x	y	z
Mo	0	0	0
P(1)	1690(2)	−1171(2)	342(2)
C(1)	3466(8)	−293(7)	441(7)
C(11a)	1714(9)	−1433(7)	1501(6)
C(12a)	2897(11)	−1097(9)	2199(7)
C(13a)	2805(12)	−1314(10)	3060(8)
C(14a)	1555(14)	−1844(10)	3225(8)
C(15a)	364(12)	−2174(9)	2527(7)
C(16a)	449(10)	−1962(8)	1683(6)
C(11b)	1867(8)	−2609(7)	−480(6)
C(12b)	2049(10)	−3542(9)	−160(7)
C(13b)	2270(11)	−4569(9)	−794(8)
C(14b)	2329(10)	−4699(9)	−1730(8)
C(15b)	2140(11)	−3769(9)	−2060(7)
C(16b)	1892(10)	−2744(8)	−1426(7)
P(2)	2277(2)	1542(2)	342(2)
C(2)	3638(8)	1011(7)	940(6)
C(21a)	3049(8)	1857(7)	−641(6)
C(22a)	4048(10)	2911(8)	−509(8)
C(23a)	4557(11)	3150(10)	−1252(9)
C(24a)	4117(11)	2375(10)	−2162(9)
C(25a)	3161(12)	1300(11)	−2346(8)
C(26a)	2638(9)	1072(9)	−1564(7)
C(21b)	2534(8)	3058(7)	1211(6)
C(22b)	3624(11)	3574(9)	1996(7)
C(23b)	3775(13)	4747(10)	2623(7)
C(24b)	2828(13)	5381(9)	2497(8)
C(25b)	1770(11)	4891(8)	1722(7)
C(26b)	1609(9)	3733(8)	1079(7)
C(31)	278(8)	822(7)	1505(6)
C(32)	535(8)	1347(7)	2393(7)
C(33)	774(10)	1948(8)	3413(6)
C(34)	985(13)	3192(11)	3808(8)
C(35)	1205(19)	3772(13)	4793(11)
C(36)	1233(21)	3126(18)	5397(11)
C(37)	1033(19)	1911(17)	5038(10)
C(38)	781(13)	1299(11)	4047(7)
thf solvent molecule *			
C(41)	6254(41)	1450(24)	4255(26)
C(42)	5389(49)	2097(34)	4905(18)
C(43)	4716(27)	2494(41)	4301(27)
C(44)	5908(29)	3142(23)	4040(25)
C(45a)	6225(44)	1977(44)	3526(28)
C(45b)	6980(45)	2577(48)	4293(32)

* C(45) is disordered over two sites, each with site occupancy 0.5.

Table 6 Electrochemical data for molybdenum and tungsten complexes[a]

Complex	${}^{I}E_{\frac{1}{2}}^{ox}$	${}^{II}E_{p}^{ox}$	$E_{\frac{1}{2}}^{red}$	Ref.
trans-[$Mo(C{\equiv}CPh)_2(dppe)_2$][b]	−0.12	0.88	−1.33	This work
trans-[$Mo(C{\equiv}CCO_2Me)_2(dppe)_2$]	−0.08	1.20	−1.40[c]	This work
trans-[$Mo(C{\equiv}CCO_2Et)_2(dppe)_2$]	0	0.69	−1.00[c]	This work
trans-[$MoCl_2(dppe)_2$]	−0.05	—	−1.68	20
trans-[$W(C{\equiv}CPh)_2(dppe)_2$]	−0.29	0.70	—	This work
[$WH_2(C{\equiv}CPh)_2(dppe)_2$]	−0.14[d]	—	—	This work
trans-[$WCl_2(dppe)_2$]	−0.24	—	−1.74	20
[$WH_2(C{\equiv}CCO_2Me)_2(dppe)_2$]	−0.02	—	—	This work
[$WH_2Cl_2(dppe)_2$]	−0.07	—	−2.4[e]	20

[a] At a platinum electrode, in 0.2 mol dm^{-3} [NBu_4][BF_4]–thf; values of potentials in volts (±0.02 *versus* SCE, measured at 200 mV s^{-1}, by using as internal reference the couple *trans*-[$ReCl(N_2)(dppe)_2$]$^{0/+}$ ($E_{\frac{1}{2}}^{ox}$ = 0.28 V *vs.* SCE). [b] A third irreversible anodic wave is observed at ${}^{III}E_p^{ox}$ = 1.11 V; a second cathodic wave is detected at −2.0 V. [c] Irreversible process; value given is for E_p^{red}. [d] Measured in a solution mixture with *trans*-[$W(C{\equiv}CPh)_2(dppe)_2$]. [e] Irreversible process; value given is for E_p^{red}.

shows the C*H*CH_2Ph resonance as a triplet at δ 5.35. These and other assignments are in Table 1.

The formation of compound **E** most probably follows a similar pathway to Scheme 2, the final step then being as in equation (2).

$$[WF({\equiv}CCH_2Ph)(dppe)_2] + HBF_4 \longrightarrow \underset{\textbf{E}}{[WF({=}CHCH_2Ph)(dppe)_2]BF_4} \quad (2)$$

Similar protonation reactions with the other alkynyl complexes did not give tractable products.

Conclusion

The precise reaction pathway and stability of intermediates in the reactions of alkynes at dinitrogen-binding metal sites is critically dependent upon the alkyne substituents and the nature of the metal site, as exemplified by the product distribution seen in this work and our observations that alkynyl complexes are not easily formed from the {$ReCl(dppe)_2$} dinitrogen-binding site.[3,24] Nevertheless, some important common features of these reactions are emerging. It is reasonable to propose that initial binding of the alkyne is followed by rearrangement to give alkynyl or vinylidene intermediates which on protonation proceed to alkylidyne and alkylidene ligands.

Further protonation to give alkyl ligands and thence alkenes (by β-hydrogen elimination) or alkanes should be attainable if the correct metal site, perhaps having more electron-releasing ligands, is used. Further experiments are planned to investigate this possibility.

Experimental

Reactions were carried out under dry dinitrogen or argon in purified solvents using standard vacuum and/or Schlenk techniques. Dinitrogen and other phosphine complexes of molybdenum and tungsten were prepared by published methods.[25] Other chemicals were used as supplied (Aldrich Chemical Company). Two 60 W tungsten bulbs were used at about 30 cm in irradiation experiments.

Infrared spectra were measured as KBr discs using a Perkin-Elmer 577 spectrometer and NMR spectra on Bruker WM360, WP80 or JEOL FX90Q instruments. Conductivities were measured using a Portland electronic bridge and cyclic voltammograms were recorded using an EG & G PAR 173 potentiostat (equipped with a 179 digital coulometer), an EG & G PARC 175 universal programmer and a Houston 2000 XY recorder, at a platinum electrode in 0.2 mol dm^{-3} [NBu_4]-

[BF$_4$]–thf. A two-compartment, three-electrode cell, with a platinum-wire working electrode, probed by a Luggin capillary connected to a silver wire pseudo-reference electrode and with a platinum or tungsten auxiliary electrode, was employed. Microanalyses were by Mr. C. Macdonald of the AFRC Nitrogen Fixation Laboratory.

trans-[Mo(HC≡CPh)$_2$(dppe)$_2$] **A**.—Phenylacetylene (0.15 cm^3) was added to *trans*-[Mo(N$_2$)$_2$(dppe)$_2$] (0.66 g) in thf (60 cm^3) under argon. The mixture was stirred at 20 °C for 24 h; the resulting solution was concentrated to 20 cm^3 in a vacuum. Slow addition of Et$_2$O (10 cm^3) precipitated a yellow solid, which was filtered off, washed with Et$_2$O (2 × 10 cm^3) and dried *in vacuo*.

[MoH$_2$(C≡CPh)$_2$(depe)$_2$] **B** (M = Mo).—The complex *trans*-[Mo(N$_2$)$_2$(depe)$_2$] (0.5 g) and PhC≡CH (0.097 cm^3, 1 mol equivalent) were stirred in thf (60 cm^3) for 27 h. The excess of solvent was then removed and the brown residue extracted with Et$_2$O. The brown, filtered extract was then reduced in a vacuum to 2 cm^3 and the brown solid product precipitated. It was recrystallised from thf–Et$_2$O as orange-brown *prisms*.

[WH$_2$(C≡CCO$_2$Me)$_2$(dppe)$_2$] **B** (M = W, R = CO$_2$Me).—The complex *trans*-[W(N$_2$)$_2$(dppe)$_2$] (1.43 g) and HC≡CCO$_2$Me (0.2 cm^3) in thf (150 cm^3) were irradiated by tungsten light whilst being stirred for 40 h. The resulting orange solution was filtered through Celite and the filtrate reduced in volume to 50 cm^3. Addition of Et$_2$O then gave an orange-red precipitate which was recrystallised from thf–Et$_2$O as red *plates*. The compound [WH$_2$(C≡CCO$_2$Et)$_2$(dppe)$_2$] was prepared in an analogous fashion.

trans-[Mo(C≡CPh)$_2$(dppe)$_2$] **C** (M = Mo, R = Ph).—Phenylacetylene (0.18 cm^3) was added to *trans*-[Mo(N$_2$)$_2$(dppe)$_2$] (0.78 g). The mixture was stirred at 20 °C for 30 h, then the resulting red solution was filtered through Celite and the red filtrate reduced to about 15 cm^3. Addition of Et$_2$O (10 cm^3) gave a red precipitate which was filtered off and recrystallised from thf–Et$_2$O as red *plates* (0.2 g). Compounds **C** (M = Mo, R = CO$_2$Me or CO$_2$Et) were prepared by a similar method.

trans-[W(C≡CPh)$_2$(dppe)$_2$] **C** (M = W, R = Ph).—The complex *trans*-[W(N$_2$)$_2$(dppe)$_2$] (2.89 g) and phenylacetylene (0.62 cm^3) were stirred in thf (200 cm^3) for 50 h under tungsten-light irradiation. The resulting orange solution was reduced *in vacuo* to 50 cm^3, Et$_2$O was added dropwise (20 cm^3) and the resulting solution stored at −5 °C overnight to afford an orange solid which was recrystallised from thf–Et$_2$O as orange *crystals*. Compounds **C** (M = W, R = CO$_2$Me or CO$_2$Et) were prepared in an analogous manner.

trans-[WF(≡CCH$_2$CO$_2$Me)(dppe)$_2$] **D**.—The salt [Et$_2$OH]-[BF$_4$] (2 mol equivalents) was added to a solution of *trans*-[WH$_2$(C≡CCO$_2$Me)$_2$(dppe)$_2$] (0.5 g) in thf (25 cm^3). The solution darkened initially to a brown colour and then lightened slightly after about 30 min. The mixture was stirred for 1 h, then the resulting yellow-brown solution was filtered through Celite and the filtrate reduced in volume to about 10 cm^3. Diethyl ether (5 cm^3) was added and the solution was stored overnight at −5 °C to give a green-yellow *solid* precipitate.

trans-[WF(=CHCH$_2$Ph)(dppe)$_2$]BF$_4$ **E**.—The salt [Et$_2$OH]-[BF$_4$] (2 mol equivalents) was added to a solution of [WH$_2$(C≡CPh)$_2$(dppe)$_2$] (0.125 g) in thf (30 cm^3) and the mixture was stirred at 20 °C for 1 h. The resulting orange solution was filtered through Celite and the filtrate was reduced to dryness, yielding an oily residue. The residue was extracted with Et$_2$O to give an orange *solid* which was filtered off, washed with thf–Et$_2$O and dried in a vacuum. Its molar conductivity in 10^{-3} mol dm^{-3} MeNO$_2$ solution was 83.1 ohm^{-1} cm^{-3} mol^{-1}.

Reactions with Acetylene. Acetylene gas was bubbled through a solution of *trans*-[M(N$_2$)$_2$(dppe)$_2$] (M = Mo or W) (0.5 g) for 10 min, then the solution was left stirring under an atmosphere of acetylene overnight. Irradiation was necessary to initiate the tungsten reaction. In both cases a black precipitate was obtained, which was filtered off, washed with Et$_2$O and dried *in vacuo*. It was identified as polyacetylene by its IR spectrum (see text) and analysis (Found: C, 92.1; H, 7.5. Calc.: C, 92.3; H, 7.6%).

Crystal Structure Analysis of [WH$_2$(C≡CCO$_2$Me)$_2$-(dppe)$_2$]·thf.—*Crystal data*. C$_{60}$H$_{56}$O$_4$P$_4$W·C$_4$H$_8$O, M = 1221.0, triclinic, space group $P\bar{1}$ (no. 2), a = 11.751(4), b = 20.737(4), c = 12.216(2) Å, α = 90.63(2), β = 102.46(2), γ = 102.74(2)°, U = 2829.5 Å^3, Z = 2, D_c = 1.433 g cm^{-3}, F(000) = 1244, μ(Mo-Kα) = 22.4 cm^{-1}, λ(Mo-K$\bar{\alpha}$) = 0.710 69 Å.

The crystals are small, bright red plates. One was mounted on a glass fibre and, after photographic examination, transferred to our Enraf-Nonius CAD4 diffractometer for determination of accurate cell parameters (from the settings of 25 reflections with θ *ca.* 10°) and measurement of diffraction intensities; before the measurement of the θ = 15–20° shell was complete the intensities of two control reflections had dropped to below 60° of their starting values and only the 2279 unique data to θ_{max} = 15° were considered reliable enough for use in the analysis. Unfortunately, no more good crystals were available. Corrections for Lorentz polarisation effects and deterioration were applied, but not for absorption.

The structure was determined by the heavy-atom method, and refined by large-block-matrix least-square methods using the SHELX program.[26] The W, P and O atoms (of the tungsten complex) were allowed anisotropic thermal parameters; the C and hydride atoms (the latter were identified in difference maps, and refined satisfactorily) were refined isotropically. The other H atoms were included in idealised positions (the methyl groups staggered), and their positional and isotropic thermal parameters were set to ride on those of their bonded C atoms. Two sites for thf solvent molecules were located, each close to a centre of symmetry; the thf molecules were disordered, occupying only one of the sites at each centre. Geometrical constraints were applied during refinement of these molecules.

Refinement was concluded with R = 0.045, R' = 0.046 for the 1927 reflections with $I > 2\sigma_I$, weighted $w = (\sigma_F{}^2 + 0.001\,34F^2)^{-1}$. The principal peaks (*ca.* 0.7 e Å^{-3}) in a final difference map were in the region of one of the thf molecules, close to atoms with high thermal parameters.

Crystal Structure Analysis for trans-[Mo(C≡CPh)$_2$(dppe)$_2$]·2thf.—*Crystal data*. C$_{68}$H$_{58}$MoP$_4$·2C$_4$H$_8$O, M = 1239.3, triclinic, space group $P\bar{1}$ (no. 2), a = 9.928(5), b = 12.086(4), c = 14.794(2) Å, α = 108.21(2), β = 96.77(3), γ = 101.36(3)°, U = 1622.3 Å^3, Z = 1, D_c = 1.268 g cm^{-3}, F(000) = 648, μ(Mo-Kα) = 3.4 cm^{-1}.

Crystals were deep red plates of irregular shape, and were found to diffract only weakly. One, *ca.* 0.31 × 0.29 × 0.10 mm, was mounted on a glass fibre, examined photographically, then transferred to our CAD4 diffractometer as above. Diffraction intensities were recorded to θ_{max} = 25° and 5700 unique reflections, corrected for Lorentz polarisation effects, absorption (by semiempirical Ψ-scan methods), and to eliminate negative net intensities (by Bayesian statistical methods), were entered into the SHELX program system.[26]

The structure was determined by the heavy-atom method (showing the Mo atom lying on a centre of symmetry) and refined by large-block-matrix least-squares methods. All non-hydrogen atoms were allowed anisotropic thermal parameters, and hydrogen atoms were included in idealised positions. A thf solvent molecule was also located, disordered in at least two orientations in which four of the atom sites are approximately common to both arrangements: the O atom was not identified.

At completion of the refinement $R = 0.103$ and $R' = 0.098$ for 4250 reflections (with $I > \sigma_I$) and a refined weighting scheme $w = (\sigma_F{}^2 + 0.004\,33F^2)^{-1}$. The only major peak, *ca.* 1.3 e Å^{-3}, in the final difference map was close to the midpoint of the Mo–C(alkynyl) bond.

The molybdenum complex was stable and many data were measured and used in the refinement process; since many of these data were 'weak' the *R* factor appears high. For the tungsten complex there were fewer intensities but they were of stronger reflections and their structure amplitudes were dominated by the W atom: hence here we were able to achieve an apparently very good *R* factor. However, the results for the former complex are rather more precise than those for the latter, as illustrated in Tables 2 and 4.

For both analyses, scattering curves for neutral atoms were taken from ref. 27. Computer programs, noted above and in Table 4 of ref. 28, were run on the VAX 11/750 system at the Agriculture and Food Research Council Institute of Horticultural Research, Littlehampton (Glasshouse Crops Research Institute).

Additional material available for both structures from the Cambridge Crystallographic Data Centre comprises H-atom co-ordinates, thermal parameters and remaining bond lengths and angles.

Acknowledgements

We thank Dr. A. Avent and Mr. C. Macdonald for NMR spectra and Instituto Nacional de Investigação Científica and Junta Nacional de Investigação Científica e Technológica (Portugal) for financial support (to M. A. N. D. A. L. and A. J. L. P.).

References

1 T. J. Katz and S. M. Hacker, *J. Am. Chem. Soc.*, 1985, **107**, 2182.

2 (*a*) M. J. Dilworth, *Biochim. Biophys. Acta*, 1966, **127**, 283; C. E. McKenna, M.-C. McKenna and C. N. Huang, *Proc. Natl. Acad. Sci. USA*, 1979, **76**, 4773; (*b*) A. J. L. Pombeiro and R. L. Richards, *Coord. Chem. Rev.*, 1990, **104**, 13.

3 N. A. Buang, D. L. Hughes, N. Kashef, A. J. L. Pombeiro and R. L. Richards, *J. Organomet. Chem.*, 1987, **323**, C47; A. Hills, D. L. Hughes, N. Kashef, M. A. N. D. A. Lemos, A. J. L. Pombeiro and R. L. Richards, *J. Organomet. Chem.*, 1988, **350**, C4.

4 H.-F. Klein, H. Beck, B. Hammerschmitt, U. Koch, S. Koppert and G. Cordier, *Z. Naturforsch., Teil B*, 1991, **46**, 147.

5 R. A. Herrick and J. L. Templeton, *Organometallics*, 1982, **2**, 843.

6 C. I. Simionescu and V. Percec, *Prog. Polym. Sci.*, 1982, **8**, 133.

7 A. A. Diamantis, J. Chatt, G. A. Heath and G. J. Leigh, *J. Organomet. Chem.*, 1975, **84**, C11.

8 R. A. Henderson, D. L. Hughes, R. L. Richards and C. Shortman, *J. Chem. Soc., Dalton Trans.*, 1987, 1115.

9 See, for example R. Goddard, J. Howard and P. Woodward, *J. Chem. Soc., Dalton Trans.*, 1974, 2025; M. I. Bruce, T. W. Hambley, M. R. Snow and A. G. Swincer, *J. Organomet. Chem.*, 1985, **235**, 105; A. Furlani, S. Licoccia, M. V. Russo, A. C. Villa and C. Guastini, *J. Chem. Soc., Dalton Trans.*, 1982, 2449; A. Blogg, A. T. Hutton, P. G. Pringle and B. L. Shaw, *Inorg. Chim. Acta*, 1983, **76**, L265; J. Geisenberger, U. Nagel, A. Sebalt and W. Beck, *Chem. Ber.*, 1983, **116**, 911.

10 A. R. Barron, G. Wilkinson, M. Montevalli and M. B. Hursthouse, *J. Chem. Soc., Dalton Trans.*, 1987, 837.

11 D. L. Hughes, A. J. L. Pombeiro and R. L. Richards, unpublished work.

12 A. Hills, D. L. Hughes, A. J. L. Pombeiro and R. L. Richards, *J. Organomet. Chem.*, 1990, **398**, C15.

13 J. Chatt, G. A. Heath and R. L. Richards, *J. Chem. Soc., Dalton Trans.*, 1974, 2074.

14 P. Meakin, L. Guggenberger, W. G. Peet, E. L. Muetterties and J. P. Jesson, *J. Am. Chem. Soc.*, 1973, **95**, 1467.

15 E. B. Lobkovski, V. D. Makhaer, A. P. Borisovach and K. N. Semenko, *J. Struct. Chem. (Engl., Transl.)*, 1980, **20**, 812.

16 H. Dadkhah, D. L. Hughes, N. Kashef, A. J. L. Pombeiro and R. L. Richards, *J. Organomet. Chem.*, 1983, **255**, C1.

17 E. L. Muetterties and L. T. Guggenberger, *J. Am. Chem. Soc.*, 1974, **96**, 1748.

18 W. Sieber, M. Wolfgruber, D. Neugebauer, O. Orama and F. R. Kreissl, *Z. Naturforsch., Teil B*, 1983, **38**, 67.

19 M. R. Churchill and W. J. Youngs, *Inorg. Chem.*, 1979, **18**, 2454.

20 T. I. Salih and C. J. Pickett, *J. Chem. Soc., Dalton Trans.*, 1985, 1255.

21 A. Hills, D. L. Hughes, A. J. L. Pombeiro and R. L. Richards, *J. Organomet. Chem.*, 1988, **352**, C5.

22 K. R. Birdwhistell, T. L. Tonker and J. L. Templeton, *J. Am. Chem. Soc.*, 1985, **107**, 4474; H. P. Kin and R. J. Angelici, *Adv. Organomet. Chem.*, 1985, **27**, 51.

23 R. Ellis, R. A. Henderson, A. Hills and D. L. Hughes, *J. Organomet. Chem.*, 1987, **333**, C6.

24 A. J. L. Pombeiro, D. L. Hughes, R. L. Richards, J. Silvestre and R. Hoffmann, *J. Chem. Soc., Chem. Commun.*, 1986, 1125 and refs. therein.

25 J. R. Dilworth and R. L. Richards, *Inorg. Synth.*, 1980, **20**, 119; A. J. L. Pombeiro and R. L. Richards, *Inorg. Synth.*, 1985, **23**, 9 and refs. therein.

26 G. M. Sheldrick, SHELX 76, Program for crystal structure determination, University of Cambridge, 1976.

27 *International Tables for X-Ray Crystallography*, Kynoch Press, Birmingham, 1974, vol. 4, pp. 99 and 149.

28 S. N. Anderson, R. L. Richards and D. L. Hughes, *J. Chem. Soc., Dalton Trans.*, 1986, 245.

Received 21*st January* 1992; *Paper* 2/00341D